G. Pozza, S. Kroesen, G. Bettella, A. Zaltron*, M. Esseling, G. Mistura, P. Sartori, E. Chiarello, M. Pierno, C. Denz, and C. Sada

T-junction droplet generator realised in lithium niobate crystals by laser ablation

Abstract: A femtosecond laser at 800 nm was used to create micro-fluidic circuits on lithium niobate ($LiNbO_3$) substrates by means of laser ablation, using different scanning velocities (100-500 μm/s) and laser pulse energies (1-20 μJ). The T-junction geometry was exploited to create on y-cut $LiNbO_3$ crystals a droplet generator, whose microfluidic performance was characterized in a wide range of droplet generation frequencies, from few Hz to about 1 kHz.

Keywords: Microfluidic; lithium niobate; laser ablation; droplet generator; T-junction

DOI 10.2478/optof-2014-0003
Received July 25, 2014; accepted September 24, 2014

1 Introduction

In the field of integrated optics Lithium Niobate ($LiNbO_3$) is a well-known crystal thanks to its good optical and structural properties, which make it a suitable material for realizing different optical components, such as light waveguides, holographic wavelength filters, Second Harmonic generators and so on [1–4]. That being so, lithium niobate is surely a promising candidate for applications also in the field of *Optofluidics*, a new research area which aims to integrate all typical lab processing on a single device, by combining the potentialities offered by optics and the tools typical of microfluidics [5]. Indeed, the passive materials most commonly used in microfluidics, like polydimethilsiloxane (PDMS) or elastomers, require the use of external equipments or the combination with various materials in order to realize the desired stages for droplet movement and optical analysis. As a matter of fact, often mechanical parts as well as external metallic electrodes have to be implemented in microfluidic devices to characterize droplets or actuate them, thus making these conventional methods less flexible and efficient than those exploiting optical approaches. Therefore, the capability to realized a microfluidic device in a material like $LiNbO_3$, where different optical stages can be easily implemented, represents a key point for promoting new insights in many applications [6, 7].

As a matter of fact, lithium niobate has been also proposed for microfluidic applications, since it is easily bondable to polymeric materials and allows for creating micropumps, by exploiting its piezoelectric properties or by realizing high efficient surface acoustic waves (SAW) generators [8, 9]. Moreover, in the last years trapping experiments have been successfully performed at the surface of lithium niobate crystals on droplets and particles dissolved in oils [10–13], by exploiting the excellent photovoltaic properties of this material, thus paving the way for its use also in the microfluidic field based on optically-driven manipulation phenomena. Quite surprisingly, all the above mentioned applications were realized simply by using a lithium niobate crystal only as active sealing layer for microfluidic circuits previously realized on PDMS, without creating the channels inside the active substrate. On the contrary, the creation of microfluidic circuits engraved on a lithium niobate crystal would significantly improve the optofluidic performances of this material, since both the integration of the optical components with the crossing fluidic channels would result more efficient and the effective volume involved in droplets actuation mechanisms would be increased. Despite of this, the realization of microfluidic channels engraved on LN has not been studied yet apart from some preliminary results where they were used standalone, i.e without any integration with physical, chemical or biological analysis stages [14, 15]. In [14] Focused Ion Beam technique was exploited to realize a microfluidic channel, but it is a slow and expensive technique and essentially useful only to fabricate nano-channels, due to its low material removal

***Corresponding Author: A. Zaltron:** Physics and Astronomy Department, University of Padua, Via Marzolo 8, 35131 Padua, Italy and Nonlinear Photonics Group, Institute of Applied Physics, University of Münster Corrensstrasse 2/4, 48149 Münster, Germany, E-mail: annamaria.zaltron@unipd.it
G. Pozza, G. Bettella, G. Mistura, P. Sartori, E. Chiarello, M. Pierno, C. Sada: Physics and Astronomy Department, University of Padua, Via Marzolo 8, 35131 Padua, Italy
S. Kroesen, M. Esseling, C. Denz: Nonlinear Photonics Group, Institute of Applied Physics, University of Münster Corrensstrasse 2/4, 48149 Münster, Germany

rate. In [15] a single straight microchannel was realized by using a polymer blade which provides optical grade dicing, but this technique is not suitable for realizing microfluidic devices with an arbitrary shape and in addition the width of each single channel is strictly conditioned by the thickness of the blade. On the contrary in this work the laser ablation technique is used, since it allows realizing fluidic circuits at the micrometer scale in a reasonable time, with any desired geometry and good quality of the channels walls, unlike the other micromachining processes mentioned above.

In this paper we present for the first time, at best of our knowledge, the realization of a microfluidic device in lithium niobate crystals by means of femtosecond laser ablation at a wavelength of 800 nm. In particular, as a proof-of-concept a droplet generator system has been fabricated, due to the recent interest of scientific community on this research area. As a matter of fact, in the last years great efforts have been directed towards the development of droplet based microfluidics, since it allows to overcome problems typical of continuous microfluidics, such as surface effects which lead to axial dispersion of liquids and the difficulty to obtain fast and efficient mixing of fluids. Moreover, each droplet can be thought as an isolated liquid compartment where chemical or biological syntheses take place, so this approach significantly reduces the risk of cross contamination between different droplets and facilitates single-cell analysis. Finally, droplet microfluidics has the ability to perform a large number of reactions without increasing device size or complexity [16] and it is characterized by a high versatility connected to the generation and manipulation of discrete droplets inside micro-devices [17]. For all the mentioned reasons and thanks to their scalability and parallel processing, droplets based systems have been used in a wide range of applications [18–21], such as the drug delivery, diagnostic testing, bio-sensing [22] and the synthesis of biomolecules such as protein and DNA [23–25]. Among the main droplet generation devices, the T-junction geometry has been chosen as reference for this work, thanks to its simple realization and the capability to produce a rich and complex scenario of stable droplets patterns ([26, 27] and references therein). The generation process of water droplets in oil, as commonly used in biological applications, is characterized and the microfluidic performances of these $LiNbO_3$ based T-junctions is discussed, demonstrating a high process reproducibility and low dispersion of droplet size distribution. These results support the exploitation of laser ablation as a suitable technique to get microfluidics device engraved in lithium niobate crystals, so that subsequent integration of several optical stages can be foreseen, thus paving the way for the realization of powerful optofluidic devices on this material.

2 Experimental

A pure y-cut $LiNbO_3$ sample with congruent composition was cut from a commercial wafer (Crystal Tech.) polished on both sides. The T-junction was realized on the + $\hat{y}$ face of the $LiNbO_3$ sample by using a Ti:Sapphire femtosecond laser (Coherent Inc.), with an operating wavelength of 800 nm, 1 kHz repetition rate and 120 fs pulse length. The laser beam was focused at the surface of the crystal by using a 50x ultralong working distance microscope objective (NA=0.55) and the workstation was equipped with a computer-controlled XYZ translation stage, which allows moving the $LiNbO_3$ sample with high spatial resolution. The addressed volume of the micro-fluidic channels was scanned successively with a resolution of 10 micron and 15 micron in the horizontal and vertical direction, respectively. The tool path was optimized to achieve flat boundaries and even surfaces. Moreover, a constant air flux was maintained at the upper surface of the sample during the micromachining process, in order to eject the ablated material out of the channels.

Several tests were performed to study the laser ablation process on lithium niobate by varying the values of scanning velocity (100-500 μm/s) and energy (1-20 μJ) used to engrave the T-junction, in order to find the best parameters to be used in our particular experimental setup. Fig. 2 illustrates the microscope images of U-grooves (200×250 μm^2) realized with the femtosecond laser by using scanning speeds equal to 100 μm/s (Fig. 2a-b-c) or 500 μm/s (Fig. 2d-e-f) and different values of the pulse energy. For each structure the bottom of the engraved areas (Fig. 2a-d), the corresponding upper edges (b-e) and the lateral views (Fig. 2c-f) are shown.

The nominal depth of the U-grooves was set to 100 μm and the images (c) and (f) in Fig. 2 clearly show that its final value strongly depends on the pulse energy used during the micromachining process, as expected since the ablation depth increases with increasing energy fluence. In particular, the effective depth was reduced by a factor of two in the U-groove realized with an energy of 1 μJ and a speed of 500 μm/s. Indeed, in this case $LiNbO_3$ is not completely crumbled and removed from the microchannel, thus preventing the further ablation of the underlying material in the micromachined area and significantly decreasing the quality of the channel walls. Although good quality microchannels could be realized with the same

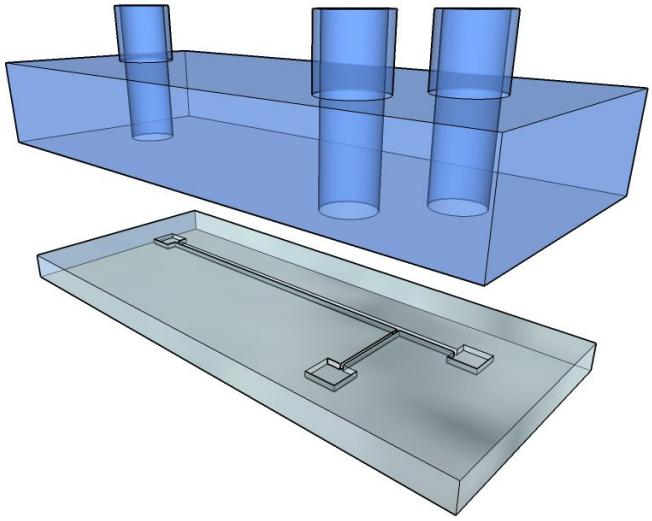

Figure 1: Scheme of the final microfluidic device: the T-junction created on the Lithium Niobate substrate and the inlet and outlet connections realized on the PDMS sealing layer are visible.

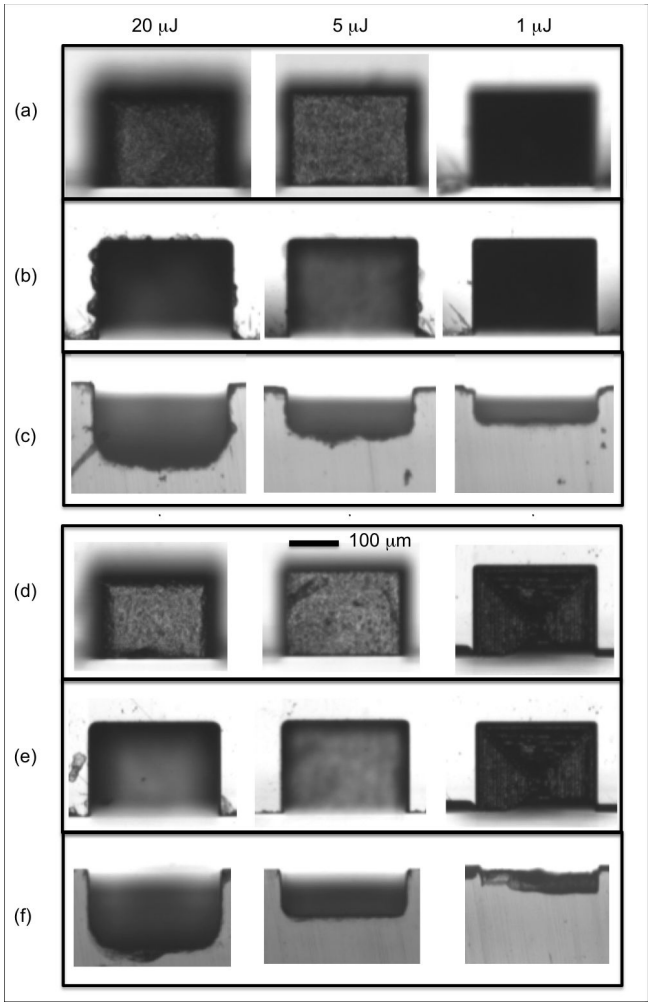

Figure 2: Microscope (40x) images of U-groove realized at the edge of a y-cut $LiNbO_3$ sample, by using scanning speeds equal to 100 μm/s (a-b-c) or 500 μm/s (d-e-f) and different values of the energy pulse. For each structure the bottom of the engraved areas (a-d), the corresponding upper edges (b-e) and the lateral views (c-f) are shown.

pulse energy of 1 μJ by simply decreasing both the scanning speed and the step between parallel lines, this will result in an extremely time-consuming process. On the contrary, the images (Fig. 2b) and (Fig. 2e) show that a slow scanning speed has to be avoided if a pulse energy of 20 μJ is used, since slivers are produced during the micromachining process resulting in scratches at the edges of the channel. This problem could be avoided by using faster scanning speeds (see Fig. 1e), but in this case the surfaces of the channel walls present more defects and irregularities and some dark debris still exist. Therefore, to shorten the preparation time of the microfluidic circuit and obtain high quality walls of the channels, the scanning speed and the energy pulse used to create the investigated T-junctions were set to 5 μJ and 500 μm/s, respectively. Moreover, the quality of the boundaries and surfaces of the ablated area were significantly improved by further scanning each final U-groove with a 4-times higher resolution.

The T-junction was then cleaned in ultrasonic baths of water, isopropanol and acetone. The scheme of the final circuit is reported in Fig. 3, where the microscope images of the inlet reservoir and the T-shape droplet generator are also shown. For the two investigated T-junctions (TJ1 and TJ2 respectively) the sizes of the three microchannels have been measured by using a surface profilemeter (KLA Tencor P-10) and the corresponding values are listed in Table 1; the reservoirs have an area of 1 mm^2 and the same depth of the microfluidic channel. The profilometer was also exploited to estimate the roughness R_a relative to the bottom of each microfluidic channel, thus comparing the obtained value with those relative to other techniques. In particular, in the analysed T-junctions the mean roughness was estimated to be R_a = (0.26 ±0.02) μm. As a matter of fact, we also tried to realize microfluidic channels by using a precision blade for optical grade dicing, but even after several optimization steps the best roughness we were able to achieve on the bottom of the channel, R_a = (0.53 ±0.01) μm, was almost a factor of two greater than the value obtained in the channels made by laser ablation. Moreover, even if the optical grade dicing showed to be a good method to realize smooth vertical walls on $LiNbO_3$ [28], this technique cannot be exploited to realize a microfluidic device with an arbitrary shape and therefore it is mainly useful to create only straight channels or waveguides. This problem can be overcome by using the

FIB technique, which allows to obtain a good roughness (few nanometers) of the channel walls, as reported in [14]. However, as already mentioned, the FIB milling process is mainly suitable for realizing nanochannels, since its material removal rate is several orders of magnitude smaller than the values typical of micromachining by femtosecond laser ablation. As a way of example, in Table 2 the main parameters relative to the fabrication process of the investigated T-junctions are summarized, where it is possible to notice that in our case the fabrication time, including both the alignment of the sample and the realization of the entire T-junction (volume equals to 5.4 x 10^8 μm^3), is less than 3 hours. On the contrary in [14] the authors report a milling time of 30 s to realize a nanochannel that is 100 μm long, 100 nm wide and 100 nm deep (volume equals to 1 μm^3). Moreover, this technique requires additional steps, such as the sputtering of a thin conductive layer on the substrate and the machine pumdown, thus significantly increasing the fabrication time. Another method often used for microstructuring of $LiNbO_3$ surface is the chemical etching process, which is also exploited to realize low-loss ridge waveguides [29]. However, this approach has three main disadvantages: the first is that the etching rate strongly depends on the crystallographic axes of the material, so that the material removal is asymmetric and the technique is useful mainly for z-cut substrates; furthermore, the maximum etching rate achievable on a lithium niobate crystal is about 1 μm/h, so that the realization of a microfluidic device with the same depth of the T-junctions used in this work would require tens of hours; finally, the chemical etching process requires to be combined with other preparation steps, such as the realization of a suitable mask at the surface of the $LiNbO_3$ substrate by means of conventional lithography, thus making the whole fabrication process more time consuming.

Even if the roughness of our T-junction does not compromise the microfluidic performances of our device, as it will be present in the following section of this paper, obviously it needs to be improved to allow combining the fluidic channels with optical components. As a matter of fact, we are currently investigating also the roughness of the lateral walls of the channels made by laser ablation, being this parameter crucial for developing optofluic devices on $LiNbO_3$. The idea is that to combine the laser ablation procedure with a post-treatment of the ablated surfaces, by means of chemical etching process or magnetorheological polishing method [30, 31], in order to recover the optical quality of the channel walls. In particular, the etching process has been already exploited in optofluidic devices realized by femtosecond laser ablation on fused silica: in [32, 33] the authors obtained a sidewall roughness

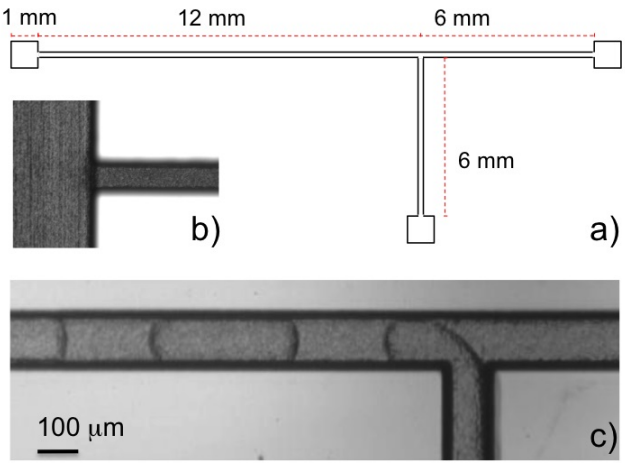

Figure 3: (a) Scheme of the final T-junction; (b) top view of the connection between the microchannel and the inlet reservoir; c) top view of the T-junction for droplet generation. The T-junction was realized with a scanning speed of 500 μm/s and energy of 5 μJ.

less than 30 nm and a larger roughness of about 200 nm on the bottom of the channels, which is comparable with our results. To this aim we prepared ad hoc microchannels, by varying both the laser ablation and the etching parameters. The characterization of the sidewall roughness of each channel was performed by means of Atomic Force Microscopy technique and all the results will be presented in a fourthcoming paper.

Finally, the two T-junctions were sealed with a thick layer of polydimethylsiloxane (PDMS), where the inlets and the outlet for the flowing liquids were previously realized (Fig. 1). To bond the lithium niobate and the PDMS surfaces, they both underwent an O_2-plasma treatment (plasma system FEMTO) for 60 s at 200 W, with an oxygen flow rate of 10 sccm at 3x10^{-3} mbar.

To test the T-junction performances, two immiscible liquids were introduced into the microfluidic devices through flexible polyethylene tubes (0.5 mm ID) by using two independent automated syringe pumps (PHD 2000, Harvard Apparatus), which allow working at constant flow rates between 1 and 500 mL/min. Hexadecane (CAS number: 544-76-3, viscosity 3cP, density 0,77 g/cm^3) and distilled water were used as continuous phase and dispersed phase, respectively [21]. The contact angle (C.A.) of both liquids on lithium niobate surface was measured: $LiNbO_3$ was completely wetted by the hexadecane (C.A.<10°) but demonstrated to be moderately hydrophobic (C.A close to 60°).

SPAN® 80 surfactant was added to hexadecane to decrease the surface energy at the water-oil interface and facilitate droplets formation [21]. The surfactant concen-

Table 1: Sizes of the microchannels for the T-junctions TJ1 and TJ2. The values of width w and depth D were obtained by using a surface profilometer. Values of the parameters α and β obtained by performing a linear fit of the data reported in Fig. 6 for the two investigated T-junctions.

T-junction	w (μm)	D(μm)	Q_C = (10.00 ± 0.04) μl/min		Q_C=(30.00 ± 0.11) μl/min	
			α	β	α	β
TJ1	126±2	89 ±6	1.44±0.01	1.68 ±0.01	1.27 ±0.05	1.54 ±0.07
TJ2	125±3	100 ±1	1.48±0.04	1.68 ±0.07	1.25 ±0.04	1.52 ±0.07

Table 2: Fabrication parameters relative to the T-junctions investigated in the present work.

fabrication time	Scanning speed	Beam diameter at 5 μJ	Translation stage resolution	Vertical/horizontal scanning step	Roughness R_a	Fabrication costs
<3 h	500 μm/s	≈ 25 μm	30 nm	15/10 μm	(0.26 ±0.02) μm	≈20-25 €/T-junction

tration was set to 1.0% (w/w) which is well above the critical micelle concentration (0.03% (w/w) for hexadecane [21, 34]. The images of the droplet generated by the T-junctions were obtained using a monochrome camera (MV D1024 CMOS, Photonfocus) coupled to an inverted microscope (Eclipse Ti-E, Nikon), whereas the videos were acquired by using the fast camera Phantom VRI v7.3.

3 Results and Discussion

The T-junction performance was tested in terms of the droplet formation frequency and droplet size distribution, by analysing with a custom made software the images extracted from videos recorded with the fast camera with a custom made software [21]. The analysed devices have a dispersed to continuous channel width ratio of 1 within 2%, a viscosity ratio of 1/3, and were tested in a range of Capillary Number (Ca) between 0.002 and 0.07; where Ca = $\mu_c v_c/\sigma$, μ_c is the viscosity of the continuous phase, v_c the velocity of the continuous phase, and σ the surface tension between the two liquids respectively [34, 35].

The droplet generation frequency f depends on the flow rates of the two immiscible liquids Q_C and Q_D, where Q_C refers to the continuous and Q_D to the dispersed phase flow rates, respectively. The highest value of f is therefore usually limited by the maximum pressure (typically a few bars) the microfluidic channels are able to sustain. In particular, in a T-junction geometry the frequency does scale in a nonlinear manner with the ratio Q_D/Q_C [34–37].

We determined the frequency f by measuring the time intervals δt between the transit of two subsequent droplets. In order to avoid bias and therefore systematic errors, the time intervals refer to distinct pairs, i.e. $\delta t_j = t_{2j} - t_{2j-1}$, where j=1...N/2 and N is the total number of droplets. Fig. 4 shows the histogram of the time intervals corresponding to the highest total flow rate achievable with our set-up, that is $Q_C + Q_D$ = 380 μl/min. The mean of this distribution yields $\Delta t_{av} = (0.864 \pm 0.001)\ ms$ which corresponds to the maximum value of the droplet generation frequency f =(1157 ±9) Hz. Moreover, by knowing the flow rate and the droplet generation frequency, it is possible to derive the volume of the droplets, which in our experiments varies between 0.8 and 2.6 nL.

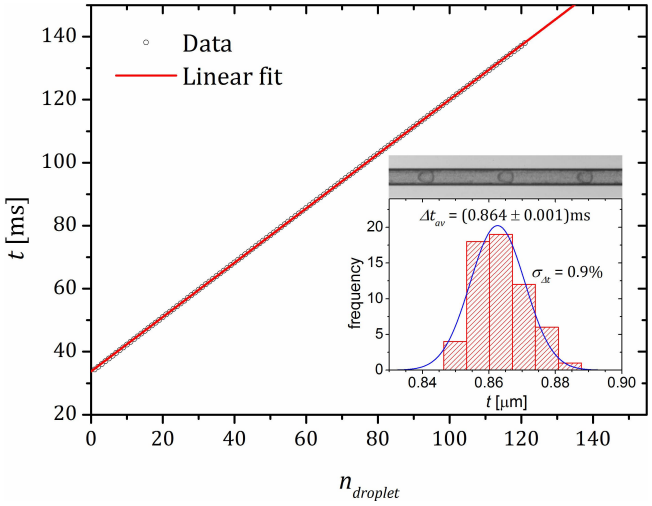

Figure 4: Examples of the measurement of the droplet formation frequency. The time interval at which each droplet passes through a reference position is reported, as a function of droplet number; the corresponding linear fit is also shown with the derived frequency of (1157 ±9) Hz. The inset presents the histogram of the time interval between subsequent droplets.

The droplet length L was estimated by analysing each droplet image extracted from a video lasting a period of time sufficiently high to obtain at least 100 droplet measurements. In particular, L was determined referring to the front and back menisci of each droplet respectively: since this procedure is affected by the grey contrast level of the recorded image, the light intensity and camera exposure time had to be properly tuned in each video recording in order to obtain the best image contrast. Fig. 5 shows an example of the histograms obtained in the case of low (a), intermediate (b) and high (c) droplet generation frequency for the T-junction TJ2, respectively. The dispersion of the length of the droplets was obtained as the standard deviation of the length distribution: in all the analysed cases it was better than 3%, in most cases lower that 2%. These values are comparable with those reported in literature [38] for T-shaped droplet generators realized with PDMS, thus highlighting the potentialities offered by $LiNbO_3$-based structures realized by laser ablation for microfluidic applications. Moreover, the three graphs clearly show that the dispersion of droplet lengths does not significantly change by increasing the droplet generation frequency in the range between 92 Hz to 1157 Hz. The fact that the dispersion values remain below 1% in all the three investigated cases confirms the good microfluidic performances of our droplet generators and the possibility to employ them also as high-frequency droplet generators.

It is worth mentioning that although the grey contrast of each video can affect the accuracy in the estimation of L by introducing a systematic error, this contribution eventually shifts the L value distribution but not its dispersion. In particular, by measuring the droplet meniscus thickness m and assuming that the values of droplet border positions follow a uniform probability density as wide as the width m, the random error σ_c in the droplet border estimation can be calculated as $m/\sqrt{12}$ [39]: the images analyses show that σ_c is about 5μm.

The production of droplets was also tested as a function of the ratio $Q_D \backslash Q_C$. In this analysis the droplets are generated in the squeezing regime, where the dynamics of their formation (break-up) is dominated by the pressure drop across the droplet as it forms [34–37]. Therefore, the length L of the droplets can be conveniently expressed with the following scaling equation

$$\frac{L}{w} = \alpha + \beta \frac{Q_D}{Q_C} \tag{1}$$

where w is the channel width and α and β are two fitting parameters, affected by the geometry of the T-junction and by the Capillary Number Ca [34–37]. In Fig. 6 we report the dependence of the ratio L/w with respect to the

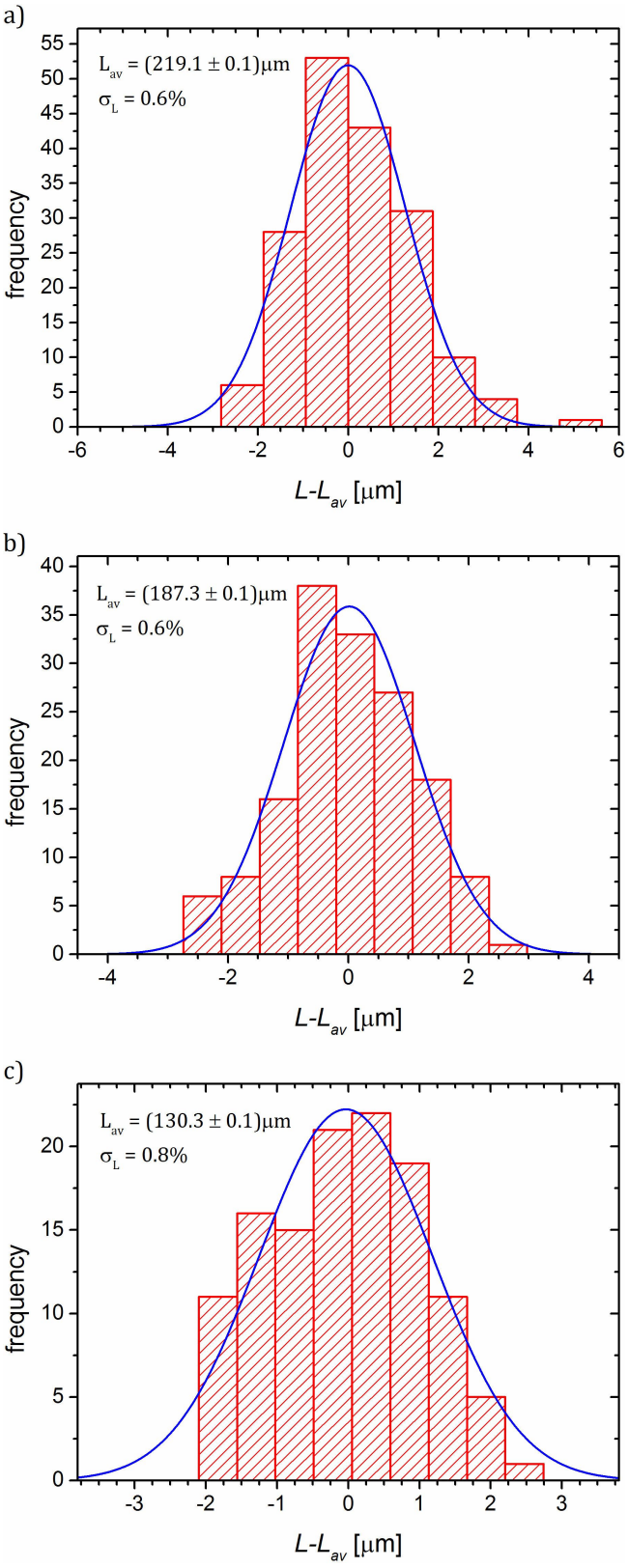

Figure 5: The histograms relative to the dispersion of the droplet length L are reported. The data were obtained in the T-junction TJ2 at a droplets generation frequency of 92 Hz (a), 467 Hz (b) and 1157 Hz (c), showing a dispersion lower than 1%.

relative flow rate Q_D/Q_C for both TJ1 and TJ2: in particular L was taken as the average value derived from one hundred droplets. The measurements were performed at two different constant values of continuous flow rate Q_C, 30 μl/min and 10 μl/min respectively, while the value of Q_D was varied between 1 μl/min and 30 μl/min. The experimental points are well fitted by a linear regression (Pearson's r value greater than 0.995), whose coefficients α and β are reported in Table 1. These results show as our T-junctions perfectly reproduce the typical microfluidic performances of T-shaped droplet generators realised with PDMS. Indeed, the linear relation between L and Q_D/Q_C was widely investigated and characterized for PDMS-based T-junctions and the results presented in [27, 40] show a good agreement with those obtained in our study. Moreover, for each value of Q_c the intercept and the slope of the linear regression are fully compatible (compatibility better than 0.3 [39]) for the two T-junctions, demonstrating the high reproducibility of the femtosecond laser technique used to realize the microfluidic device in the $LiNbO_3$ substrate.

On the contrary, in Fig. 6 it is evident that both the values of α and β vary with the flow rate Q_c of the continuous phase. However, this difference is forecasted by Eq. 1, since the parameters α and β depend not only on the geometry of the channels, which is almost the same in graphs (a) and (b), but also on the capillary number of the microfluidic device, which in turn increases with increasing Q_c, especially in the case of a high viscosity ratio [34–37].

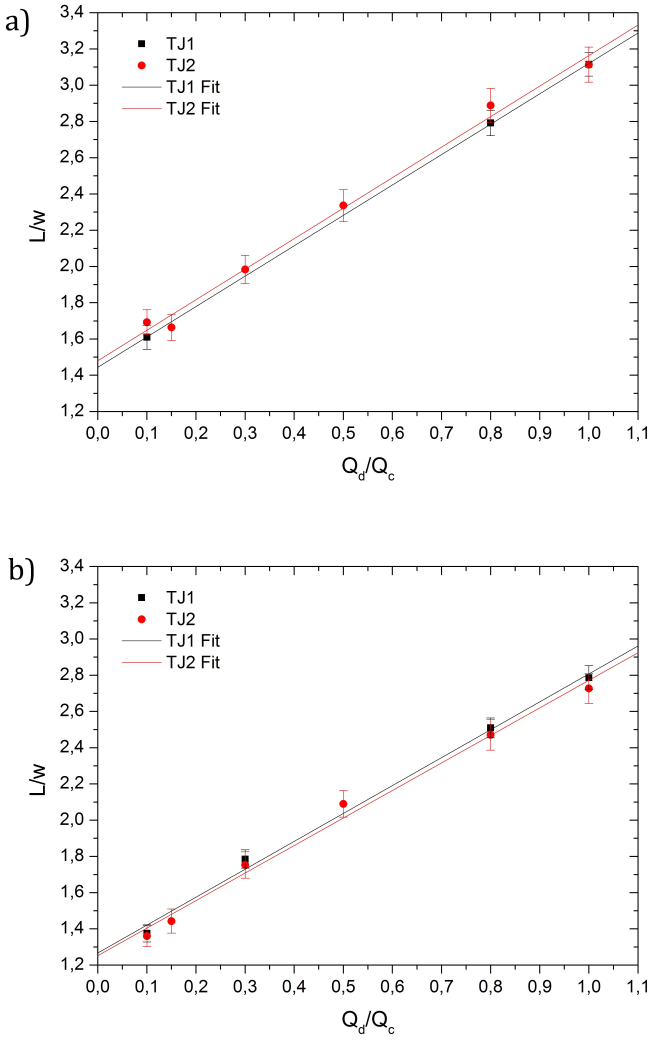

Figure 6: The values of L/w are reported as a function of the ratio between the dispersed and continuous flow rates, Q_D/Q_C. The value of Q_C is fixed to 10 μl/min (a) or 30 μl/min (b), while the value of Q_D is properly varied. The straight lines represent the linear fits of the experimental data, for both TJ1 and TJ2.

4 Conclusion

Laser ablation with femtosecond laser operating at a wavelength of 800 nm has been demonstrated to be a suitable technique to get high performant microfluidic channels engraved in lithium niobate crystals. In particular we showed that among the different scanning velocities (100-500 μm/s) and laser pulse energies (1-20 μJ) exploited, the best results were obtained at 500 μm/s and 5 μJ. With this technique we have realized T-junctions in $LiNbO_3$ chips sealed by a PDMS layer. The microfluidic performances of these devices were characterized in a wide range of droplet generation frequencies, from a few Hz to about 1 kHz. The droplet length distribution was analysed at different frequencies and showed a low dispersion with a standard deviation less than 3%. The microfluidic performance of different T-junctions realized on lithium niobate suggests that laser ablation guarantees a high reproducibility and good quality channel shape. Therefore, this approach paves the way toward a direct integration on a single $LiNbO_3$ substrate of passive micro-fluidic devices and active optical components, like waveguides, holographic filters and droplet actuators driven by light.

Acknowledgement: The authors kindly acknowledge the Ca.Ri.Pa.Ro foundation for financing the research by the Excellence Project "Integrated opto-microfluidic prototype on lithium niobate crystals for sensing applications" (call 2011-2012) and the COST action MP1205 "Advances in Optofluidics: Integration of Optical Control and Photonics with Microfluidics".

Finally the author M.Pierno kindly acknowledges the European Research Council under the Europeans Commu-

nity's Seventh Framework Programme (FP7/2007-2013) / ERC Grant Agreement N. 297004 (DROEMU) and P. Mistura the University of Padova within the project PRAT2011 "MINET".

References

[1] C. Denz, K.-O. Müller, T. Heimann, and T. Tschudi, "Volume holographic storage demonstrator based on phase-coded multiplexing", *IEEE Journal of Selected Topics in Quantum Electronics* 4, 1998, 832

[2] S. Breer and K. Buse, "Wavelength demultiplexing with volume phase holograms in photorefractive lithium niobate", *Applied Physics B* 66, 1998, 339

[3] Y. L. Lee, N. E. Yu, C. Jung, B.-A. Yu, I.-B. Sohn, S.-C. Choi, Y.-C. Noh, D.-K. Ko, W.-S. Yang, H.-M. Lee, W.-K. Kim and H.-Y. Lee, "Second-harmonic generation in periodically poled lithium niobate waveguides fabricated by femtosecond laser pulses", *Applied Physics Letters* 89, 2006, 171103

[4] M. Carrascosa, M. Cabrera and F. Agulló-López, "Long-Lifetime Photorefractive Holographic Devices via Thermal Fixing Methods", *Infrared Holography for Optical Communications* 86, 2003, 91

[5] L. Pang, H. M. Chen, L. M. Freeman and Y. Fainman, "Optofluidic devices and applications in photonics, sensing and imaging", *Lab on Chip* 12, 2012, 3543

[6] D. Psaltis, S. R. Quake and C. Yang, "Developing optofluidic technology through the fusion of microfluidics and optics", *Nature* 442, 2006, 381

[7] M. L. Y. Sin, J. Gao, J. C. Liao and P. K. Wong, "System Integration - A Major Step toward Lab on a Chip", *Journal of Biological Engineering* 5, 2011, 1

[8] M. F. Schneider, Z. Guttenberg, S. W. Schneider, K. Sritharan, V. M. Myles, U. Pamukci and A. Wixforth, "An Acoustically Driven Microliter Flow Chamber on a Chip (μFCC) for Cell–Cell and Cell–Surface Interaction Studies", *A European Journal of Chemical Physics and Physical Chemistry* 9, 2008, 641

[9] J. Friend and L. Y. Yeo, "Microscale acoustofluidics: Microfluidics driven via acoustics and ultrasonics", *Reviews of Modern Physics* 83. 2011, 647

[10] H. A. Eggert, F. Y. Kuhnert, and K. Buse, "Trapping of dielectric particles with light-induced space-charge fields", *Applied Physics Letters* 90, 2007, 241909

[11] M. Esseling, A. Zaltron, N. Argiolas, G. Nava, J. Imbrock, I. Cristiani, C. Sada and C. Denz, "Highly reduced iron-doped lithium niobate for optoelectronic tweezers", *Applied Physics* B 113, 2013, 191

[12] M. Esseling, A. Zaltron, C. Sada and C. Denz, "Charge sensor and particle trap based on z-cut lithium niobate", *Applied Physics Letters* 103, 2013, 061115

[13] M. Jubera, A. García-Cabañes, J. Olivares, A. Alcazar, and M. Carrascosa, "Particle trapping and structuring on the surface of $LiNbO_3$:Fe optical waveguides using photovoltaic fields", *Optics Letters* 39, 2014, 649

[14] M. Sridhar, D. K. Maurya, J. R. Friend and L. Y. Yeo, "Focused ion beam milling of microchannels in lithium niobate", *Biomicrofluidics* 6, 2012, 1

[15] M. Chauvet, L. Fares and F. Devaux, "Self-trapped beams for fabrication of optofluidic chips", Proceedings of SPIE 8434, 2012, 84340Q-1

[16] H. Song, D. L. Chen and R. F. Ismagilov, "Reactions in Droplets in Microfluidic Channels", *Angewandte Chemie International Edition* 45, 2006, 7336

[17] K. Jensen and A. Lee, "The science and applications of droplets in microfluidic devices", *Lab on Chip* 4, 2004, 31N

[18] V. Chokkalingam, B. Weidenhof, M. Krämer, W. F. Maier, S. Herminghaus and R. Seemann, "Optimized droplet-based microfluidics scheme for sol-gel reactions", *Lab on Chip* 10, 2010, 1700

[19] C. N. Baroud, M. R. de Saint Vincent, and J. P. Delville, "An optical toolbox for total control of droplet microfluidics," *Lab on Chip* 7, 2007, 1029

[20] J.C Baret, V.Taly, M. Ryckelynck, C. A. Merten, A.D. Griffiths, "Droplets and emulsions: very high-throughput screening in biology", *Medicine Science* 25, 2009, 627

[21] E. Piccin, D. Ferraro, P. Sartori, E. Chiarello, M. Pierno and G. Mistura, "Generation of water-in-oil and oil-in-water microdroplets in polyester-toner microfluidic devices", *Sensors and Actuators B* 196, 2014, 525

[22] P. Watts and S. J. Haswell, "The application of micro reactors for organic synthesis", *Chemical Society Reviews* 34, 2005, 235

[23] V. Noireaux and A. Libchaber , "A vesicle bioreactor as a step toward an artificial cell assembly", Proceeding of National Academy of Sciences U. S. A. 101, 2004, 17669

[24] M. S. Long, C. D. Jones, M. R. Helfrich, L. K. Mangeney-Slavin, and C. D. Keating, "Dynamic microcompartmentation in synthetic cells" Proceeding of National Academy of Sciences U. S. A. 102, 2005, 5920

[25] H. J. Choi and C. D. Montemagno, "Biosynthesis within a bubble architecture", *Nanotechnology* 17, 2006, 2198

[26] A. Gupta and R. Kumar, "Effect of geometry on droplet formation in the squeezing regime in a microfluidic T-junction", *Microfluidics and Nanofluidics* 8, 2010, 799

[27] P. Garstecki, M. J. Fuerstman, H. A. Stone and G. M. Whitesides," Formation of droplets and bubbles in a microfluidic T-junction-scaling and mechanism of break-up", *Lab on Chip* 6, 2006, 437

[28] N. Courjal, B. Guichardaz, G. Ulliac, J.-Y. Rauch, B. Sadani, H.-H. Lu, M.-P. Bernal,"High aspect ratio lithium niobate ridge waveguides fabricated by optical grade dicing" *Journal of Physics D: Applied Physics* 44, 2011, 305101

[29] H. Hu, R. Ricken, W. Sohler and R. B. Wehrspohn, "Lithium niobate ridge waveguides fabricated by wet etching", *IEEE Photonics Techology Letters* 19, 2007, 417

[30] P. Sivarajah, C. A. Werley, B. K. Ofori-Okai, K. A. Nelson, "Chemically assisted femtosecond laser machining for applications in LiNbO3 and LiTaO3", *Applied Physics* A, 2013, 112

[31] J-W. Lee, Y.-K. Cho, M.-W. Cho, G.-H. Kim and T.-J. Je, "Optical transmittance recovery of powder blasted micro fluidic channels on fused silica glass using MR polishing", *International Journal of Precision Engeneering and Manufacturing* 13, 2012, 1925

[32] R. Osellame H. J. W. M. Hoekstra, G. Cerullo and M. Pollnau, "Femtosecond laser microstructuring: an enabling tool for optofluidic lab-on-chips", *Laser Photonics Reviews* 5, 2011, 442

[33] V. Maselli, J. R. Grenier, S. Ho and P.R. Herman, "Femtosecond laser writtien optofluidic sensor: Bragg grating waveguide evanescent probing of microfluidic channel", *Optic Express* 17, 2009, 11719

[34] R. Seemann, M. Brinkmann, T. Pfohl, and S. Herminghaus, "Droplet based microfluidics", *Report on Progress in Physics* 75, 2012, 016601

[35] C.N. Baroud, F. Gallaire and R. Dangla, "Dynamics of microfluidic droplets" *Lab on Chip* 10, 2010, 2032

[36] J.H. Xu, S. W. Li, J. Tan, Y. J. Wang, and G. S. Luo, "Controllable Preparation of Monodisperse O/W and W/O Emulsions in the Same Microfluidic Device, *Langmuir* 22, 2006, 7943

[37] J.H. Xu, S. W. Li, J. Tan and G. S. Luo, "Correlations of droplet formation in T-junction microfluidic devices: from squeezing to dripping", *Microfluidics Nanofluidics* 5, 2008, 711

[38] V. Steijn, C. R. Kleijn and M. T. Kreutzer, "Predictive model for the size of bubbles and droplets created in microfluidic T-junctions" *Lab on Chip* 10, 2010, 2513

[39] Bureau International des Poids et Mesures, Evaluation of measurement data – Guide to the expression of uncertainty in measurement, (2005)

[40] G. F. Christopher, N. N. Noharuddin, J. A. Taylor and S. L. Anna, "Experimental observations of the squeezing-to-dripping transition in T-shaped microfluidic junctions", *Physical Review E* 78, 2008, 036317-1